SUBCORTICAL NETWORK PROPERTIES IN PARKINSON'S DISEASE

BY

JARED HESSE

A Thesis Submitted to the Graduate Faculty of

WAKE FOREST UNIVERSITY GRADUATE SCHOOL OF ARTS AND SCIENCES

in Partial Fulfillment of the Requirements

for the Degree of

MASTER OF ARTS

Psychology

May, 2016

Winston-Salem, North Carolina

Approved By:

Dale Dagenbach, Ph.D., Advisor

Wayne E. Pratt, Ph.D., Chair

Paul J. Laurienti, M.D., Ph.D.

Christian E. Waugh, Ph.D.

ACKNOWLEDGMENTS

I would like to thank everyone that helped make this thesis possible. All of the assistance I received from the great people at school, the Laboratory for Complex Brain Networks, and from the Wake Forest Baptist Medical Center is irreplaceable. The present study could not be completed without the help from these wonderful researchers, faculty, and scientists.

At the LCBN, I would like to thank Paul Laurienti, Robert Lyday, and Debra Hege. Robert's skills in MATLAB and other analytical tools were invaluable to turning any ideas I had about data analysis into realities. Paul has helped me think critically about network science in ways I could have never conceptualized, and to not accept halfway explanations for fully realized phenomena. I am grateful to have worked with such brilliant researchers during my time here.

At the hospital, I would like to extend thanks to Ihtsham Haq, Robert Coghill, and everyone else in my lab. Ihtsham has guided me through understanding the complexities and subtleties of Parkinson's disease, and shown me what it takes to work in a lab that strives to make a real difference in people's lives. He routinely challenges me to work harder, and to think more critically. Working with him and the rest of my lab at the hospital has proven to be an invaluable experience.

At Wake Forest, I am indebted to the guidance that I have received from Dale over the past two years. I have truly had a transformative experience as a scholar, and as a person. Despite only having an initially tangential interest in network applications to brains, I became fascinated and enamored with understanding the brain as a complex network. Through everything, Dale has been a stalwart adviser. Additionally, I would like

to thank my committee members, Wayne Pratt and Christian Waugh, for guiding me through my entire thesis process. Their perspectives have helped shape my writing and presentation immensely. I have them to thank for the improved clarity, coherency, and linearity of my writing; a critical tool in clearly communicating the jumble of ideas I have.

Lastly, to those I hold close to me, and to those I love: thank you Peter, Jane, Megan, and Heather. It would have never happened without you.

TABLE OF CONTENTS

LIST OF TABLES

LIST OF FIGURES

ABSTRACT

Parkinson's disease has been characterized as a "disconnection syndrome" reflecting the disruption of neural pathways. Network science analyses provide a promising way of further analyzing this characterization given the rich data they provide about the interrelationships between brain areas. In this study, network science graph theory based analyses were performed using the resting state data from 14 individuals with Parkinson's disease.

The networks consisted of 90 nodes defined in natural brain space for each individual. Global efficiency and local efficiency were calculated. The mean global and local efficiencies for the 10 subcortical nodes and for the remaining 80 nodes were then correlated with an array of behavioral measures: the Barrett Impulsivity Scale (BIS), Beck Depression Inventory (BDI), and the Montreal Cognitive Assessment (MOCA). Subcortical global and local efficiency were significantly correlated with all three scales; positively in the case of the BIS and BDI (in which higher scores imply worse symptomology) and negatively in the case of the MOCA (in which lower scores imply worse symptomology).

These preliminary analyses suggest further explorations of brain connectivity using the tools of networks science may enhance our understanding of what occurs in Parkinson's and how that is reflected in behavioral disruptions.

INTRODUCTION

Parkinson's disease is a neurodegenerative disorder that currently affects an estimated seven to ten million people worldwide, with one million cases in the United States. The disease is an economic burden with the combined direct and indirect cost estimated to be around 25 billion dollars per year in the United States alone (Parkinson's Disease Foundation, 2016). The disorder is primarily characterized by its three most common motor symptoms: an at-rest tremor, bradykinesia, and rigidity or stiffness of the limbs. Other motor symptoms include freezing of gait, drooling, dystonia, and a flat affect. Additionally, certain nonmotor symptoms such as olfaction loss, depression, sleep disturbances, and mood disorders are common with the disease, and can at times precede diagnosis by years.

Although little is known about the direct cause of the disease, its pathology has been extensively studied. It is characterized by the death of dopaminergic neurons in the substantia nigra, but the exact mechanism that begins this process of cell death is unknown. The substantia nigra is a neural structure located in the midbrain that is part of a system of primarily subcortical nuclei called the basal ganglia. The other structures in the basal ganglia are the striatum (putamen), interior and exterior globus pallidus (pallidum), and the subthatlamic nucleus. The basal ganglia are thought to be responsible for regulating planned motor movements (Knierim, 2016).

The basal ganglia are part of a neural circuit that forms a critical role in Parkinson's disease. The substantia nigra has subcortical dopaminergic projections that form multiple neural pathways, called the motor, limbic, and associative circuits. The motor loop, which is of importance to Parkinson's, has two dopaminergic pathways that

begin in the substantia nigra pars compacta, called the direct and indirect pathways (see Figure 1). In healthy patients both pathways are ultimately responsible for stimulating the motor cortex through the ventral thalamus, and the disruption of this function is thought to be responsible for several of the primary symptoms of Parkinson's disease.

The direct pathway begins with an excitatory D1 projection from the substantia nigra pars compacta to the striatum, which then forms an inhibitory connection to the interior globus pallidus, which has an inhibitory connection to the ventral thalamus, which then has an excitatory link to the motor cortex. When this pathway is stimulated, the striatum disinhibits the ventral thalamus through the interior globus pallidus, and the thaalmus then stimulates the motor cortex.

When dopamine acts on the D2 receptors of the substantia nigra pars compacta, it inhibits striatal activity instead of exciting it. This is the start of the indirect pathway, which begins with an inhibitory connection from the striatum to the exterior globus pallidus. Next, there is another inhibitory conncetion from the exterior globus pallidus to the subthalamic nucleus, and an excitatory branch from the exterior globus pallidus to the interior. The end result of striatal inhibition causes stimulation of the motor cortex through thalamic disinhibition via the interior globus pallidus, much like the direct pathway. The indirect pathway also passes through the subthalamic nucleus to the interior globus pallidus. In healthy patients the subthalamic nucleus's excitatory connection to the interior globus pallidus is normally inhibited by the exterior globus pallidus.

The primary motor symptoms of Parkinson's disease are thought to be a byproduct of the dysfunction in the motor loop while several of the nonmotor symptoms in Parkinson's disease occur due to the overall loss of available dopamine. When the

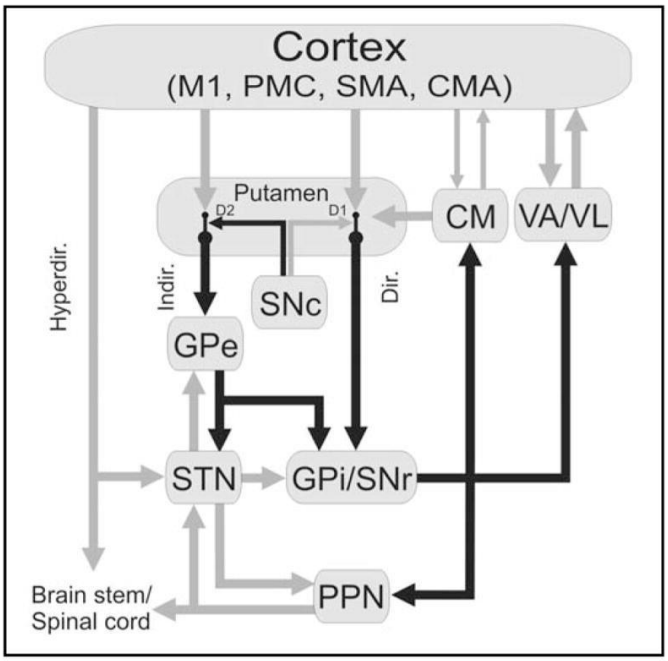

Figure 1. Motor circuit of the basal ganglia. CM = centromedian nucleus of the thalamus, VA/VL = Ventral anterior/ventrolateral nucleus of the thalamus. Black connections are inhibitory, and grey connections are excitatory. From DeLong and Wichmann (2010).

dopamine producing neurons in the substantia nigra die, its excitatory and inhibitory effects on the striatum are lost, and this causes disruption in the motor circuit.

In the indirect pathway the loss of dopamine significantly diminishes the inhibitory effect of the striatum on the exterior globus pallidus, whose inhibitory connection on the subthalamic nucleus is subsequently weakened. This causes excessive excitation of the interior globus pallidus from the subthalamic nucleus, which in turn will now excessively inhibit the ventral thalamus. This causes pathological under-excitation from the ventral thalamus to the motor cortex, and is thought to be responsible for difficulties planning movements in Parkinson's.

The direct pathway to the ventral thalamus is also affected by the overall loss of dopamine. Without the excitatory D1 projection from the substantia nigra to the striatum,

striatal inhibition of the interior globus pallidus is weakened. This causes the interior globus pallidus to have a stronger inhibitory effect on the ventral thalamus which will now activate the motor cortex less than it should. The irregular functioning of these pathways to the motor cortex is thought to be responsible for the bradykinetic, freezing, and tremor symptoms in Parkinson's. (Lee, Chau, & Leong, 1995).

The symptoms of Parkinson's disease do not manifest until 60 to 80% of the dopamine producing neurons in the substantia nigra die (National Parkinson's Foundation, 2016). The Braak staging hypothesis claims that this is explained by the first pathologies of Parkinson's disease occurring in the olfactory bulb before spreading into the substantia nigra (Braak et al., 2003). This claim is substantiated by research that has found Lewy body accumulation in the olfactory bulb during early stages of the disease, and that the loss of either smell or taste is considered a potential early indicator of Parkinson's (Davie, 2008). One of the primary risk factors for Parkinson's is the manifestation of these Lewy bodies throughout the cortex. Lewy bodies are misfolded, filamentous proteins composed of alpha-synuclein whose abnormal buildup also plays a role in other dementias (Lang, 1998). Over 90% of Parkinson's cases are characterized by the presence of Lewy bodies, but their detection is limited to post-mortem (Lee & Trojanowski, 2006). Without a reliable way to detect the presence of Lewy bodies in-vivo, the subsequent most well-documented risk factors for the disease are having a first-degree relative with Parkinson's, being above the age of 60, sleep disorders, and the previously mentioned loss of smell or taste.

Because of the unclear causal effects leading to the disease, and the inability to measure Lewy body presence, one goal of contemporary Parkinson's research is to find

reliable methods of early detection. A strong possibility is that there may be structural or functional changes predictive of Parkinson's that can be measured using neuroimaging methods. Neuroimaging methods have been extensively used in order to extract reliable biomarkers from other neurodegenerative disorders such as Huntington's and Alzheimer's disease, (Dickerson et al., 2011; Paulsen et al., 2014; Rosenberg et al., 2015).

For some diseases, it has been possible to look at the size of important cortical and subcortical structures in diseased brains in order to ascertain volumetric change due to atrophy. But, due to the size of the subcortical structures involved in Parkinson's disease, conventional magnetic resonance imaging (MRI) has poor contrast when imaging fine areas like the substantia nigra and the rest of the basal ganglia, therefore volumetric assessment is problematic. For the same reason, these areas must be "traced", or segmented, with precision from each participant's anatomical structure when examining group differences between them. The subtleties and gross differences in segmentation methods and MRI contrasts have led to numerous papers in the Parkinson's literature making contradictory claims regarding the volume of the substantia nigra (Pyatigorskaya et al., 2014).

More recently, a number of studies have tried to examine neural changes in Parkinson's disease using network analyses of functional connectivity based on functional MRI (fMRI) resting state data. fMRI relies on BOLD signal oscillations in the brain to provide the basis for functional activity. BOLD oscillations are considered to be a strong proxy for neural activity, and at rest they represent the intrinsic activity of the brain. Resting-state scans involve no task and take place over a period where the

participant is usually told to remain relaxed while staring at a fixation point. Resting-state fMRI is a strong candidate for studying Parkinson's disease from this standpoint as the beginning stages of the disease are entirely characterized by neural and functional modifications that cannot be detected by traditional imaging methods. Resting-state fMRI also fits well with Parkinson's from a pragmatic standpoint, as it does not rely on complicated tasks that may involve motor coordination and can also be easily deployed.

In a resting-state functional connectivity network, nodes are typically defined by brain tissue, and their connections are defined by the temporal correlation of the BOLD signal. The size of a node in contemporary research can range from the size of a 4x4x4 mm cube to as large as whole anatomical regions taken from a brain atlas. During the time of acquisition, usually approximately five minutes, correlations between low-frequency BOLD signal oscillations from the selected regions of the brain are used to order to construct a functional network. Pairwise correlations between all the nodes in the functional network are used to generate an association matrix. This association matrix is then binarized according to a set connectivity threshold. This threshold's purpose is to remove noise, in the form of low correlated functional areas, from the network. This association matrix is then mapped back onto a standardized brain space and analyzed using network science measures (Bullmore & Sporns, 2009).

Functional connectivity analyses of Parkinson's disease have generated a number of insights. For instance, Helmich and colleagues (2010) have characterized Parkinson's in terms of a loss of functional connectivity in the brain. The researchers defined a region's connectivity by its degree, the network metric *k*, which is a summation of a node's or region's incoming and outgoing connections. They found an overall loss of

connectivity in the striatum, brainstem, midbrain, pons and cerebellum in the Parkinson's group, compared to controls. The loss of connectivity in these particular regions is thought to be tied to the expression of symptoms that are related to each region.

Other functional connectivity studies of Parkinson's have observed differences in whole brain metrics. For example, specific network efficiency measures called global and local efficiency differentiate patients from controls. In network science, global efficiency (E_{glob}) and local efficiency (E_{loc}) are commonly used to characterize the information transfer efficacy of the brain[1]. E_{glob} is calculated using the average inverse shortest path length (inverse of *L*), and is a measurement of the parallel information transfer efficiency of a network. The less "jumps" it takes from one node in the network to get to any other *x* node, the higher the global efficiency. E_{loc} is a measure of information transfer efficiency calculated within local subgraphs; it is defined as the inverse of the shortest average path length of all neighbors of a given node. Another way of thinking about local efficiency is that it a measure of how well any node's connections are connected to each other.

Of particular interest to Parkinson's disease, Achard and Bullmore (2007) conducted a repeated-measures experiment where dopamine receptor antagonists were administered to healthy participants after an initial resting-state scan. The researchers

[1]Calculating efficiency in a network. First, the average efficiency *E* of any network *G* is calculated. *N* denotes the total nodes in a network, and *d* (*i*, *j*) represents the shortest path between any two nodes (*i*, *j*). Local efficiency uses G_i, which consists of only node *i*'s immediate connections. Global efficiency uses G^{ideal}, which is the number of all possible connections between nodes in a network. From Latora & Marchiori, (2001).

$$E(G) = \frac{2}{n(n-1)} \sum_{i<j \in G}^{n} \frac{1}{d(i,j)}$$

$$E_{glob}(G) = \frac{E(G)}{E(G^{ideal})} E_{loc}(G) = \frac{1}{N} \sum_{i \in G}^{n} E(G_i)$$

found that the participants' whole-brain global and local efficiency was significantly lower after the dopamine antagonist was administered. Skidmore et al. (2011) expanded on this finding by comparing Parkinson's patients in the "OFF" medicine state to controls, and found similar effects of decreased global and local efficiency.

Recent research by Wei et al. (2014) explored this even further in Parkinson's disease by performing a specific regional analysis on the structures involved in the basal ganglia loop. Global efficiency scores for the supplementary motor area, primary motor cortex, primary somatosensory cortex, thalamus, globus pallidus, and putamen were all significantly decreased compared to controls, and these efficiencies were also significantly negatively correlated with UPDRS (Unified Parkinson's Disease Rating Scale) scores ($r = -0.44$, $p < .01$). The UPDRS is the most widely-used diagnostic measure of Parkinson's disease progression, with higher scores signifying a stronger disease burden. In the context of this study, this means that the low global efficiency scores in the study's predefined basal ganglia loop network were related to Parkinson's patients having worsened symptoms. Given the importance of dopamine to this circuit, these results show that as the disease progresses and symptoms worsen, the functional efficacy of the basal ganglia motor loop degrades in kind.

However, an important caveat for this research, and several other studies of global and local efficiency in Parkinson's (Baggio et al., 2014; Luo et al., 2014; Zhang et al., 2015), is that the patients were scanned in the "OFF" medicine state, where there is already an implication of reduced dopaminergic functioning. This makes sense given the goal of finding patterns that could be used as early predictor's of Parkinson's.

But it may also be informative to determine what connectivity patterns are like in the Parkinson's brain while "ON" medication. At the time of writing there is currently no "ON" medication study of global and local efficiency in Parkinson's from a whole-brain, as well as a subcortical, perspective. Similar functional connectivity studies of Parkinson's disease that have participants in the "ON" state do not report global or local efficiency metrics (e.g., Göttlich et al., 2013; Wu et al., 2009).

Repeating this analysis "ON" medicine may inform us about the effects of treatment: Does medication reverse the subcortical changes in global and local efficiency completely, partially, or does its effect reflect actions occurring elsewhere in the brain? Is the degree of change in subcortical global and local efficiency while "ON" medication related to disease state outcomes? The present study fills this gap in the literature because it has participants in the "ON" state while performing similar analyses of efficiencies and their relationships to clinical outcomes, such as UPDRS scores, on a whole-brain and strictly subcortical level. We hypothesized that participants' global efficiency and local efficiency scores will be normalized due to the administration of levodopa, and that subcortical efficiencies will not normalize; they will still be lower and strongly correlate with disease burden and other clinical outcomes.

In addition to looking at subcortical global and local efficiency, the present study also examines changes in community structure that occur in Parkinson's disease. Communities in a network are groups of nodes that are more internally connected to each other than they are externally. Dubbelink and colleagues (2013) conducted a longitudinal study of brain network topology changes in Parkinson's disease over time, including community analyses. They found that community structure within the Parkinsonian

networks decreased over time. This means that the functional networks began to appear more random over time in terms of their connections, as the communities broke down.

Therefore, as time progresses we can expect the communities of long-since diagnosed patients to look very dissimilar to newly diagnosed patients, as communities weaken. It is important to consider the fact that time and disease progression do not increase in a one-to-one ratio, and that this study was time-based and not disease-stage based. Even though communities decline over time, there's no indication of how this degradation is related to disease progression. If a link between disease progression and community structure was found it could potentially reliably discriminate between Parkinson's stages. Additionally, there may be group differences in community structure that may discriminate patients from controls.

Community structure has frequently been studied in Parkinson's disease using the network metric of modularity (Baggio et al., 2014; Göttlich, 2013; Lebedev et al., 2014). Modularity is an algorithm that detects communities by calculating "the number of edges falling within groups minus the expected number in an equivalent network with edges placed at random," and is also posited as the definitive way to detect communities (Newman, 2006). The communities generated by modularity are called modules.

On an individual level, the number of modules that are generated in the context of resting-state fMRI networks will almost always be different. One participant could have twelve modules at rest, while another could only have five. They are inherently unique. Therefore, differences in modules between groups must be explained using methods that do not rely on averaging. Averaging modules would involve collapsing individual modularity maps into a group image and comparing two of these images to see where

there is, or is not, overlap. As modules will undoubtedly cover different structural and functional areas, collapsing modules together across a group by averaging creates a very misleading picture.

The present study addresses this problem by comparing how modular the networks are, any differences in the number of modules, and how modular participation of subcortical nodes between groups differs. These three methods involved analyzing correlations and group differences using a network statistic called *Q*, examining module counts in both groups, and running a specialized permutation procedure first used by Alexander-Bloch and colleagues (2012).

In order to compare modularity between groups, a specific metric for it must be chosen. How modular a network is can be quantified in terms of the network statistic *Q*. *Q* is a statistic that is calculated using the proportion of a network's connections that fall within modules, subtracted by the proportion that would be expected due to random chance. *Q* can be thought of as a goodness-of-fit measure for a network's modularity, as a higher *Q* means that the current modular structure is getting closer to the best possible fitting model. It is important to emphasize that a high *Q* does not imply a higher number of modules. It is only indicative of increasing degrees of model fit.

Group differences in the modularity of networks were can assessed by comparing *Q* values. *Q* was also compared to disease progression and clinical outcomes within the Parkinson's group in order to discover any possible relationships between them. We hypothesized that *Q* values would be negatively related to disease burden based on prior research and the assumption that "cross-talk" increases as a function of disease.

Group differences in the number of modules can also be compared. As mentioned earlier, there is no recognized positive or negative value associated with the number of modules a person has, but there may be an underlying pattern to the number generated that may differentiate Parkinson's patients from controls or be related to disease burden.

Lastly, differences in the modular participation of subcortical nodes were assessed using a method proposed by Alexander-Bloch et al., (2012) that allows for determining whether the nodes that modules are comprised of differ significantly between groups. Differences in a node's functional community would inform us about how the discrete organization of the brain at rest is different between Parkinson's patients and controls, and could be demonstrative of an underlying biomarker. We hypothesized that the structure of modules that included subcortical nodes would differ for some subcortical nodes between patients and controls.

These hypotheses are based on research that describes potential integrative connectivity between the subcortical regions and other regions of the brain in Parkinson's. One such study, conducted by Wu et al., (2009), found decreased functional connectivity in the putamen and supplementary motor area and increased connectivity in the globus pallidus. Overall connectivity was measured by the net number of incoming and outgoing connections to the region. The researchers offer compensatory connection as a possible explanation: As the putamen and supplementary motor area begin to function abnormally, the globus pallidus and other subcortical structures may be becoming more functionally connected to external areas in order to make up for this deficit.

This theory of functional compensation has been corroborated by new contributions to the Parkinson's literature (Zhang et al, 2015). For example, in Parkinson's, decreases in functional connectivity between the caudate and putamen have been found to be related to hyperconnectivity (defined as having higher connections than controls) in the surrounding motor areas (Vervoort et al., 2016). Furthermore, functional connectivity analyses of walking studies have shown that Parkinson's patients utilize cognitive resources, found in the form of novel functional connections, to compensate for gait-specific deficits (Maidan et al., 2016). Still, these studies were performed when patients were in the "OFF" state. The current study assessed how functional compensation may manifest in the "ON" state.

In sum, the current study examined whole-brain and exclusively subcortical global and local efficiency scores of Parkinson's patients in the "ON" medicine state. These scores were compared between groups, and related within the Parkinson's group to disease progression and clinical outcomes. We hypothesized that participants' global efficiency and local efficiency scores would not differ on a whole-brain scale, but would when examining the subcortical nodes. In addition, we also theorized that subcortical global and local efficiencies would strongly correlate with negative disease outcomes.

Differences in how modular participants' networks were assessed using *Q*, and we hypothesized that *Q* would be inversely related to disease burden in the Parkinson's group as evidence suggests that "cross-talk" between disparate functional regions becomes necessary in advanced disease stages. Similarly, the number of modules in participants' networks were compared between groups, and related to disease burden in the Parkinson's group. Lastly, module participation of subcortical nodes was contrasted

between groups using the permutation procedure described in Alexander-Bloch et al., (2012). It was hypothesized that some subcortical nodes would differ in their module participation, as a function of group.

Before getting into the detailed methods, one further challenge must be mentioned. Due to significant atrophy in the brains of the current study's Parkinson's patients, the AAL (Automated Anatomical Labeling) atlas had to be reverse-warped onto all participants' native space brains in order to create 90-node networks. Native space networks are not registered to any anatomical template. Although this sacrifices fidelity somewhat, the advantage of using an atlas in this context is that it allows for accurately studying advanced-stage brains without the possibility of creating unrepresentative data.

As Parkinson's disease progresses there is a general loss of white matter throughout the brain, especially in the frontal areas. (Tessitore et al., 2015). This can make creating accurate functional networks difficult as resting-state fMRI relies on a certain level of "intactness" of the brain's white matter for the purpose of warping and coregistration to predefined anatomical spaces. If the brain has too significant a level of atrophy then attempting to register it to standard space can be thought of as similar to trying to enlarge a small image: the less pixels there are to begin with, the fuzzier and distorted the end result looks to be. This issue has been discussed somewhat in the literature, and a more conservative approach to network creation and registration is favored as being closer to the "true" underlying network (Magalhães et al., 2015).

There is a precedent for working with native space brains in the functional connectivity literature, and they are not so uncommon that they are perceived as

methodologically inferior or atypical. Certain studies suggest that native space analyses may afford better fidelity than standard space registrations in regards to ROI analyses.

Hutchison and colleagues (2014) compared analyses of group differences when using standard versus native space ROIs during a digit-symbol verification task. ROIs for the prefrontal motor cortices were generated in both native and standard space. The researchers found that standard space ROIs would more often inflate or minimize group differences. This is thought to be due to the natural variations in each person's neural anatomy. Indeed, several studies have suggested that matching functional data to an individual's structural data can ultimately give the most accurate analysis (Fischl et al., 2008, Seibert & Brewer, 2011 & Seibert et al., 2012).

The AAL is a brain atlas developed by Tzourio-Mazoyer and colleagues (2002) that parcellates the brain into 90 distinct anatomical areas of interest. The AAL is generally seen as a macro-atlas insofar as it divides the brain into larger pieces than other atlases. The AAL atlas is the chosen node parcellation scheme for the current study. Although it is not the most widely used atlas, it has several advantages over more popular atlases, such as the MNI (Montreal Neurological Institute atlas), using Broadmann's areas, and Talairach coordinates, especially in the context of the present study. For instance, Talairach coordinates have become the de facto method for identifying brain regions, even after brains are registered to different standard spaces. This causes discrepancies in regional identification, and frequently Talairach coordinates will point to the "wrong" region (Chau & McIntosh, 2005).

Due to the abundance of different network parcellation methods available in the literature, Zalesky and colleagues (2010) conducted an analysis to determine whether or

not the choice of node parcellation schemes matters in whole-brain networks. This is a crucial question, as the best definition of a node in a large brain network hasn't been defined explicitly, unlike in social network analysis, for example, where a node is a person or organization and an edge represents some sort of direct relationship.

The researchers found that comparisons of network metrics across studies that used different parcellation methods (e.g., different atlases) but had the same spatial scale (number of nodes) were consistent to the point of only about a 3% variation. However, when different spatial scales were used, features such as small-worldness were changed by up to 95%. This is important as it shows that the current study must be limited in its comparison to other studies of a similar spatial scale. The upside is that the atlas is a real representation of the functional network across studies as long as the spatial scale, in this case a whole-brain scale, remains the same. This means that the AAL atlas used in this study makes it comparable to recent whole-brain AAL Parkinson's studies such as Lebedev et al., (2014).

Numerous functional imaging studies, especially in the context of neurodegenerative diseases, have utilized the AAL in network construction. The AAL's popularity with neurodegenerative work is more than likely due to its macroscopic nature. Several atlases with hundreds of parcellated regions make working with diseased brains difficult. Expected cortical and subcortical landmarks may not be located where they are supposed to be, whether it be due changes from advanced age that is often correlated with these diseases, or due to the atrophy that also frequently occurs. In the case of neurodegenerative disease, less is certainly more. For instance, the AAL was used by Khazaee, Ebrahimzadeh, & Babajani-Feremi (2015) in a functional imaging study of

Alzheimer's disease that accurately classified AD patients using a machine learning algorithm derived from each participant's functional network. As a further testament to its credibility, the AAL has also been used in several seminal functional network papers, including Achard et al., (2006), Achard AND Bullmore (2007), and Liu et al., (2008).

METHODS

Participant Demographics

The current study was composed of 28 participants: 14 in the Parkinson's group, and 14 as controls. Three additional Parkinsonian participants were initially discarded due to severe head motion in the scanner. The study group was composed of 11 male and 3 female persons with clinical Parkinson's disease who were right-handed, non-demented and were not significantly cognitively impaired at the time. The age range was from 50-80 years (M = 66.42, SD = 8.52), with an average disease duration of 4.25 years. The Parkinson's group data was taken from an unpublished functional imaging study on impulsivity in Parkinson's conducted by the Wake Forest Baptist Medical Center. Each participant was scanned in the "ON" state of medication. Patients' medications were converted to the approximate levodopa dosage to standardize them. The participants and controls were all matched for gender, handedness, education (presence of an advanced degree), and age (±2 years).

Additionally, each patient also had several associated behavioral and clinical measures. Patients' UPDRS scores were used as the primary measure of disease burden. Current levodopa dosage, Barrett Impulsivity Scale (BIS) scores, Beck Depressive Inventory (BDI) scores, and Montreal Cognitive Assessment (MOCA) scores were all used as ancillary measures. First and second-order BIS subscales were also used in all correlational analyses in order to tap into specific domains of impulsive behaviors. MOCA scores could not be located for five patients, and UPDRS "OFF" scores at the time of scanning were not readily available for four patients. Descriptive statistics for these scales can be found in Table 1.

Each scale and subscale of the BIS relates to a specific hypothesized domain of impulsivity. The primary measures are of attentional, motor, and nonplanning impulsivity. Broadly speaking, they refer to the ability to attend to appropriate stimuli, the ability to inhibit motor movements, and the ability to plan for the future, respectively. The three second-order scales, Attentional, Motor, and Nonplanning, each contain two of the first-order scales, as they further elaborate on the proposed facet of impulsivity. Attentional has Attention and Cognitive Instability, Motor has Motor and Perseverance, and Nonplanning has Self-Control and Cognitive Complexity.

Table 1

Parkinson's Group Clinical & Behavioral Scores

	N	*Mean*	*SD*
BIS Total	14.00	56.00	9.31
BDI Total	14.00	8.78	5.54
MOCA Total	9.00	26.33	2.64
UPDRS "ON"	14.00	22.07	6.09
UPDRS "OFF"	10.00	27.00	9.20
Levodopa Dosage (mg)	14.00	485.42	269.65
Disease Duration (Years)	14.00	4.25	3.01
BIS Attentional	14.00	14.57	3.08
BIS Motor	14.00	19.64	2.95
BIS Nonplanning	14.00	20.50	7.76
BIS Attention	14.00	9.35	2.49
BIS Cognitive Instability	14.00	5.21	1.25
BIS Motor	14.00	12.78	2.51
BIS Perseverance	14.00	6.85	0.86
BIS Self-Control	14.00	11.00	4.20
BIS Cognitive Complexity	14.00	10.78	2.15

The control group was created using archived resting state data scans from various studies conducted by the Laboratory for Complex Brain Networks (LCBN). The

age range was also 50-80 years (M = 66.42, SD = 8.52). All controls were healthy, non-demented, right-handed, and not experimentally manipulated somehow (e.g., an alcoholic abstaining from alcohol before a resting-state scan). The control group did not have any equivalent tests to the clinical and behavioral ones used in the Parkinson's group. Table 2

Table 2

Participant Demographics – By Group

	N	*Percentage*
Parkinson's		
Gender		
Male	11.0	79%
Female	3.0	21%
Race		
White	14.0	100%
Education (Years)		
<12	0.0	0%
12-16	10.0	71%
16+	4.0	29%
Control		
Gender		
Male	11.0	79%
Female	3.0	21%
Race		
White	14.0	100%
Education (Years)		
<12	0.0	0%
12-16	12.0	85%
16+	2.0	15%
	M	*SD*
Parkinson's		
Age	66.29	8.40
Control		
Age	66.42	8.52

includes demographics for all participants. As education and age could not be matched on a strictly one-to-one level, two t-tests were conducted on education and age in order to ensure that the controls were appropriately matched. These are presented in the Results section.

Image Acquisition and Network Construction

All participants were scanned using a 3T Siemens MR scanner at the Wake Forest Baptist Medical Center. The scanning protocol varied from study to study for controls and patients across the entire session, but the same initial resting-state scan was always used (Scan time ~ 5 minutes, TR = 2.0s). All fMRI data were used to create brain networks in native space. Networks that had been previously collected at a 4x4x5mm were resliced to 4x4x4mm before processing. These data were preprocessed using SPM8. Scan time spent on signal equilibration was determined and subsequently discarded for all participants. Functional images were realigned, slice-time corrected, and co-registered to a skull-stripped version of the participants' associated structural data. Structural data were parcellated into gray matter, white matter, and cerebrospinal maps using the unified segmentation function in SPM8. Functional data was also motion-corrected to eliminate scan volumes with excessive frame-wise displacement and BOLD signal change (Power et al., 2012).

Due to significant cortical atrophy in the Parkinson's patients' brains, all participant scans were kept in native space instead of being registered to an anatomical template. As a replacement, the Automated Anatomical Labeling atlas (AAL) was reverse-warped onto participants' native space networks in order to create 90 node networks. The accuracy of the warp for each participant was visually examined to ensure

its correctness. Functional brain networks were generated from a correlation matrix of time series data from each node pair using the Pearson correlation coefficient. Additionally, only positive connections in the network were kept as they are most relevant to the current study; negative interregional correlations have been shown to alter network statistics and overall network topology (Schwarz & McGonigle, 2011; Wang et al., 2011).

Network connections were then thresholded at 4% in order to maximize *Q* for each network and to eliminate any spurious temporal correlations. Past analyses have found that these analyses will be robust at a 4% threshold, and, given that there is no currently best accepted value for thresholding, this fixed threshold approach gave us the most idealized level of modularity while also maintaining a fixed average degree across the network. (Alexander-Bloch et al., 2012; Simpson, Bowman, & Laurienti, 2013).

Analyses of Network Statistics

Global and local efficiency scores were compared on both a whole-brain and subcortical level. Efficiency scores for the whole- brain regions were calculated on a nodal level using Dijkstra's algorithm, found in the Brain Connectivity Toolbox used by Rubinov and Sporns (2010). The current study defines ten subcortical nodes as the Left and Right Amygdala, Putamen, Caudate, Pallidum, and Thalamus. Anatomical and functional regions of interest that are too fine to study, such as the substantia nigra and globus pallidus, are subsumed by these nodes. These nodes were chosen due to their level of anatomical correspondence to the primary areas of dysfunction in Parkinson's disease. The cerebellum was excluded from all analyses.

Global and local efficiencies for these nodes were averaged for each participant to get average scores for each in the subcortical region. Global and local efficiency scores for the remaining nodes were averaged to get scores representing cortical nodes. Mean group differences in both whole-brain and strictly subcortical efficiencies were assessed using t-tests. In addition, each of the individual subcortical nodal efficiencies were contrasted between the Parkinson's and control groups.

In the Parkinson's group correlations between these efficiencies and UPDRS, BDI, BIS, levodopa dosage, and MOCA scores were calculated.

Modularity Analyses

The current study utilized a method first presented in Alexander-Bloch et al. (2012) to assess differences in the modular assignment of subcortical nodes between groups. This was done using a specialized permutation procedure. This procedure first determines what other nodes are a member of a given node *X*'s module. All nodes are then relabeled to reflect this: a 1 signifies membership, and a 0 means non-membership. This is calculated for each node in each network. These matrices are then compared across groups using Pearson's phi, which is a measure of association between two dichotomous variables bounded between -1 and 1, with zero signifying no relationship. Phi is calculated as a goodness-of-fit measure for a 2x2 contingency table, and how it would look in this case is described in Figure 1. The average phi coefficient is calculated after this is ran for each node in the network.

Genuine differences can then be assessed via a permutation procedure that compares the within-group average phi coefficient to data that has the group membership of each node randomized. If the within-group average phi is higher than the randomly

assigned data it is indicative of a genuine difference in the functional community between groups. This shuffling procedure is performed 10,000 times to ensure accuracy, and the error rate is controlled using an FDR (false discovery rate) correction. In the current study, this procedure is hypothesis-driven, and will only use the 10 subcortical nodes defined by the AAL, instead of the entire network: the left and right Thalamus, Amygdala, Putamen, Pallidum, and Caudate.

	Node X_1	**Node X_2**
# of Nodes That Are A Member Of X's Module	**10**	**15**
# of Nodes That Are Not A Member Of X's Module	**80**	**75** $\varphi = \sqrt{\frac{\chi^2}{n}}$

Figure 2. A visual example of how a phi coefficient is calculated. Phi equals the square root of the chi square test of this contingency table divided by the number of counts.

Next, how modular participants' networks were assessed using *Q*. For the within-group Parkinson's analysis, *Q* was correlated with UPDRS, BDI, BIS, levodopa dosage, and MOCA scores. The between groups analysis consisted of a t-test to determine if a mean difference in *Q* existed. The most widely used function for calculating modularity comes from Newman & Girvan (2004): the proportion of a network's edges that fall within modules, subtracted by the proportion that would be expected due to random chance alone (*Figure 3*).

Lastly, differences in the counts of modules were evaluated. The within-group analysis in Parkinson's disease correlated the number of modules with UPDRS, BDI, BIS, levodopa dosage, and MOCA scores. Module counts were also correlated with

cortical and subcortical efficiency in both groups order to ascertain any possible relationships. Another t-test was conducted to determine the existence of any mean differences in the number of modules between groups.

$$Q(G, \text{Part}) = \frac{1}{2\text{m}} \sum_{i \neq j} (A_{\text{ij}} - P_{\text{ij}})\, \delta\,(M_i, M_j)$$

Figure 3. Q is a function of a graph (G) and partitions of G's nodes into modules (Part). M is the total number of edges. Aij = 1 if an edge links i and j, or it is zero. δ (M_i, M_j)=1 if i and j are in the same module, or it is zero. Pij is the probability that there would be an edge between i and j, given a random graph with the same degree distribution as the graph. Pij is calculated as the product of nodes i and j's degree over the total number of edges in the network.

Top Overlap Images

As part of our exploratory analysis, top overlap maps for E_{glob} and E_{loc} were generated. Top overlap maps are generated by taking a predefined percentage of nodes for a given network statistic and then overlaying the within-group consistency of these nodes on a standardized brain space. That is, each overlap map shows the amount of consistency in the location of the top percentage nodes within each group. However, this analysis must be framed as exploratory, due to the fact that the overlap maps have been warped to a standardized template, from their native space, for the purposes of this analysis.

In the present study the top 20% highest $E_{glob\ and}$ E_{loc} nodes were used, and their overlap maps were then generated. This allows for a qualitative examination of the consistency of high efficiency nodes across the brain, and between groups.

RESULTS

Demographic Differences

Two t-tests were run comparing age and years of education between the Parkinson's patients and the control group. They revealed no significant differences in age or education between the experimental groups, $t(26) = -.045$, $d = -0.01$, $p > .05$, $t(26) = -.852$, $d = -.33$, $p > .05$.

Differences in Whole-Brain and Subcortical Efficiencies

The network statistics across the entire brain and for cortical and subcortical areas separately for the Parkinson's group are presented in Table 3. The same statistics for the control group are presented in Table 4. Ten nodes were defined as subcortical, and the remaining 80 were used for the cortical nodes.

Table 3

Network Statistics for Parkinson's Group

	M	*SD*
Whole-Brain E_{glob}	0.17	0.03
Whole-Brain E_{loc}	0.46	0.04
Cortical E_{glob}	0.17	0.02
Cortical E_{loc}	0.46	0.05
Subcortical E_{glob}	0.16	0.05
Subcortical E_{loc}	0.45	0.23
Average Degree (*K*)	3.60	0.00
Q	0.70	0.03
# of Molecules	18.92	4.20

There were no significant group differences in whole-brain global efficiency, $t(26) = -.431$, $d = -.17$, $p > .05$, or local efficiency, $t(26) = .156$, $d = .06$, $p > .05$. Additional t-tests revealed that there were no significant mean differences in subcortical global and local efficiency, $t(26) = 1.19$, $d = .47$, $p > .05$, $t(26) = .690$, $d = .27$, $p > .05$. Two final t-tests failed to show a significant group difference in cortical global efficiency, $t(26) = -.077$, $d = -.03$, $p > .05$, or local efficiency, $t(26) = -.838$, $d = -.33$, $p > .05$. These results indicate the absence of group differences in efficiencies between controls and "ON" medicine Parkinson's patients, at-rest. These results are consistent with the hypothesis of efficiency "normalization" caused by levodopa.

Table 4

Network Statistics for Control Group

	M	*SD*
Whole-Brain E_{glob}	0.17	0.04
Whole-Brain E_{loc}	0.46	0.03
Cortical E_{glob}	0.17	0.04
Cortical E_{loc}	0.47	0.03
Subcortical E_{glob}	0.14	0.06
Subcortical E_{loc}	0.40	0.19
Average Degree (*K*)	3.60	0.00
Q	0.72	0.04
# of Molecules	19.64	2.87

The previous analyses were based on using values averaged across all nodes, all subcortical nodes, or all cortical nodes for each participant. Because of the distinct

possibility that different subcortical nodes would be reconfigured differently, additional t-tests were performed to determine whether differences between Parkinson's and the control group existed for any of the individual subcortical nodes. The results of these are shown in Table 5.

Out of the conducted t-tests, four showed significant differences. For the Parkinson's group, the Right Caudate and Left Pallidum had significantly higher E_{glob}, $t(26) = 2.36$, $d = .92$, $p < .05$, $t(26) = 2.25$, $d = .88$, $p < .05$ and the Left and Right Thalamus also had significantly higher E_{loc} than the control group, $t(26) = 2.31$, $d = .90$, $p < .05$, $t(26) = 2.50$, $d = .98$, $p < .05$.

Table 5

Analyses of Individual Subcortical Nodes

Parkinson's Group	*M (SD) E_{glob}*	*M (SD) E_{loc}*
Amygdala L	.13 (.12)	.41 (.45)
Amygdala R	.12 (.03)	.29 (.43)
Caudate L	.17 (.10)	.37 (.39)
Caudate R	.17 (.09)	.40 (.46)
Putamen L	.20 (.54)	.41 (.40)
Putamen R	.20 (.08)	.41 (.45)
Pallidum L	.18 (.07)	.43 (.43)
Pallidum R	.19 (.08)	.50 (.42)
Thalamus L	.17 (.10)	.51 (.41)
Thalamus R	.14 (.11)	.54 (.44)

Control Group	*M (SD)* E_{glob}	*M (SD)* E_{loc}
Amygdala L	.13 (.10)	.41 (.47)
Amygdala R	.19 (.09)	.54 (.42)
Caudate L	.14 (.09)	.20 (.29)
Caudate R	.08 (.10)	.28 (.45)
Putamen L	.18 (.09)	.61 (.36)
Putamen R	.20 (.07)	.62 (.30)
Pallidum L	.11 (.10)	.50 (.46)
Pallidum R	.15 (.08)	.44 (.48)
Thalamus L	.10 (.09)	.17 (.36)
Thalamus R	.10 (.08)	.16 (.34)

T-Test Results	$t(E_{glob})$	$d(E_{glob})$	$t(E_{loc})$	$d(E_{loc})$
Amygdala L	-0.01	0.00	0.06	0.02
Amygdala R	-1.96	-0.76	-1.56	-0.61
Caudate L	0.79	0.30	1.28	0.50
Caudate R	2.36*	0.93	0.75	0.29
Putamen L	0.67	0.26	-0.45	0.36
Putamen R	-0.14	0.02	-1.00	0.30
Pallidum L	2.25*	0.88	-0.43	-0.16
Pallidum R	1.22	0.48	0.38	0.15
Thalamus L	1.89	0.74	2.31*	0.90
Thalamus R	1.19	0.46	2.50*	0.98

* $p < .05$. ** $p < .01$.

Whole-Brain and Subcortical Relationships to Clinical Outcomes

Consistent with our hypothesis, whole-brain efficiency measures were not significantly correlated with any of the behavioral or clinical outcomes, nor were strictly cortical areas. These correlations can be found in Tables 6, 7, 8, and 9.

Table 6

Correlations Between Whole-Brain Efficiencies and Clinical Outcomes

	M *(SD)*	BIS	BDI	MOCA[†]	UPDRS ON	UPDRS OFF[††]
E_{glob}	0.17 (.03)	.473	.526	-.283	.126	-.006
E_{loc}	0.46 (.04)	0.25	.145	.145	.122	-.459

* $p < .05$. ** $p < .01$. [†]N = *9*. [††]*N* – 10. *N* = 14 for all other measures.

Table 7

Correlations Between Whole-Brain Efficiencies and BIS Subscales

	Attentional	Motivation	Non-Planning	Attention	Cognitive Instability	Motor	Perseverance	Self-Control	Cognitive Complexity
E_{glob}	.198	.437	.111	.179	.131	.454	.170	.215	.056
E_{loc}	-.190	-.423	.460	-.297	.127	-.362	-.388	.441	.097

* $p < .05$. ** $p < .01$.

Table 8

Correlations Between Cortical Efficiencies and Clinical Outcomes

	M *(SD)*	BIS	BDI	MOCA[†]	UPDRS ON	UPDRS OFF[††]
E_{glob}	0.17 (.03)	.364	.428	-.144	.152	.035
E_{loc}	0.47 (.04)	-.486	-.271	.658	.122	-.075

* $p < .05$. ** $p < .01$. [†]N = *9*. [††]*N* – 10. *N* = 14 for all other measures.

Table 9

Correlations Between Cortical Efficiencies and BIS Subscales

	Attentional	Motivation	Non-Planning	Attention	Cognitive Instability	Motor	Perseverance	Self-Control	Cognitive Complexity
E_{glob}	.101	.335	.081	.087	.075	.377	.045	.157	.066
E_{loc}	-.466	-.074	.460	-.076	-.133	-.307	-.069	-.139	-.222

* $p < .05$. ** $p < .01$.

When examined on a subcortical level, these relationships dramatically changed. Table 10 and 11 show correlations between the clinical and behavioral outcomes and subcortical efficiencies in Parkinson's, as well as correlations with specific BIS subscales. Subcortical global and local efficiency were significantly positively correlated with BIS (Barrett Impulsivity Scale) scores and BDI (Beck Depressive Inventory) scores ($p < .01$). Additionally, both were also significantly negatively correlated with MOCA

Table 10

Correlations Between Subcortical Efficiencies and Clinical Outcomes

	M (*SD*)	Subcor. E_{loc}	BIS	BDI	MOCA†	UPDRS ON	UPDRS OFF††
Subcor. E_{glob}	0.16 (.05)	.569*	.731**	.720**	-.911**	-.023	-.184
Subcor. E_{loc}	0.45 (.23)		.820**	.647*	-.679*	-.075	-.466

* $p < .05$. ** $p < .01$. †$N = 9$. ††$N = 10$. $N = 14$ for all other measures.

(Montreal Cognitive Assessment) scores (p <.01). Higher BIS and BDI scores indicate greater impulsivity and depression respectively, while lower MOCA scores are associated with decreased cognitive functioning.

Table 11

Correlations Between Subcortical Efficiencies and BIS Subscales

	Attentional	Motivation	Non-Planning	Attention	Cognitive Instability	Motor	Perseverance	Self-Control	Cognitive Complexity
Subcor. E_{glob}	.509	.683**	.191	.477	.301	.596*	.597*	.366	.783**
Subcor. E_{loc}	.817**	.139	.787**	.807**	.400	-.031	.562*	.864**	.499

* p < .05. ** p < .01.

The correlations between the individual scales of the BIS and the subcortical efficiencies are presented in Table 11. Subcortical E_{glob} was significantly positively correlated with the second-order Motivation factor (p < .01), and the first-order Motor, Perseverance (p < .01), and Cognitive Complexity (p < .05). Additionally, Subcortical E_{loc} was significantly positively correlated with the second-order Attentional and Non-Planning factors (p < .01), and the first-order Attention, Perseverance (p < .05), and Self-Control factors (p < .01).

The relationships found in Tables 10 and 11 show that greater subcortical global and local efficiency is directly related to the severity of impulsivity, depression, and impaired cognitive functioning in Parkinson's. Based on the compensation hypothesis in

Parkinson's, high global and local efficiency could be related to higher integration between subcortical and cortical regions. In turn, greater compensatory connections may be associated with the presence of more disease related symptoms in terms of impulsivity, depression, and cognitive functioning. However, without corresponding behavioral data for the control group, this has to remain a speculation.

For the same reasons presented earlier, and to ascertain if any one node or nodes were driving these relationships, these correlations were also run on the nodal level, instead of using the average efficiencies of the 10 nodes. These results can be found in Table 12. The results show that the individual subcortical nodes generally follow a similar pattern, in terms of direction, to their correlations on the average level. At the individual node level, the correlations between global efficiency of the left amygdala and thalamus and the BDI, and the right amygdala and right thalamus and the BIS are significant (p <.05). The global efficiency of the left and right thalamus also correlates with cognitive functioning. Local efficiency of the left caudate is correlated with cognitive functioning, while local efficiency of the right caudate is correlated with both the BIS (p < .01) and BDI (p < .05). Local efficiency of the left pallidum is correlated with cognitive functioning, while that of the left thalamus is correlated with the BIS (p <.05). These findings should be viewed cautiously due to the number of tests performed.

Overall, the pattern of correlations suggests that the efficiencies associated with the caudate, pallidum, thalamus, and amygdala are related to the behavioral measures of impulsivity, depression, and cognitive functioning. Given the significant mean differences in nodal efficiencies found between the caudate, pallidum and the thalamus between Parkinson's patients and controls, these results seem to imply that they are the

nodes in which changed efficiencies may be related to deficits in these behaviors in the Parkinson's group. Analogous behavioral measures for the control group would help solidify the existence of this possibility.

Table 12

Correlations Between Individual Subcortical Nodes and Clinical Outcomes

(E_{glob})	*M (SD)*	BIS	BDI	MOCA	UPDRS ON	UPDRS OFF
Amygdala L	.13 (.12)	.459	.567*	-.398	-.006	.026
Amygdala R	.12 (.10)	.544*	.511	-.625	-.383	-.446
Caudate L	.17 (.10)	.278	.408	-.759	-.084	.136
Caudate R	.17 (.09)	.358	.295	-.389	.267	-.001
Putamen L	.20 (.08)	.480	.378	-.311	-.041	-.485
Putamen R	.20 (.08)	.489	.347	.097	.167	.098
Pallidum L	.18 (.07)	.442	.316	-.566	-.126	-.541
Pallidum R	.19 (.09)	.469	.345	-.304	.157	.091
Thalamus L	.17 (.10)	.529	.635*	-.732*	-.200	-.324
Thalamus R	.14 (.11)	.569*	.609*	-.684*	.147	-.003

(E_{loc})	*M (SD)*	BIS	BDI	MOCA	UPDRS ON	UPDRS OFF
Amygdala L	.42 (.46)	.459	.266	-.182	-.165	-.324
Amygdala R	.29 (.43)	.072	.149	-.399	.154	.184
Caudate L	.37 (.39)	.526	.413	-.691*	.018	-.150
Caudate R	.40 (.46)	.566*	.642**	-.176	.231	-.108
Putamen L	.55 (.40)	.310	.169	-.212	.131	-.321
Putamen R	.49 (.40)	.513	.220	-.128	.150	-.185
Pallidum L	.44 (.43)	.513	.465	-.686*	-.268	-.575
Pallidum R	.50 (.42)	.476	.281	-.442	.041	-.307
Thalamus L	.51 (.41)	.545*	.481	-.422	-.197	-.507
Thalamus R	.54 (.44)	.513	.436	-.129	-.478	-.540

* $p < .05$. ** $p < .01$.

Top Overlap Maps of E_{glob} and E_{loc}

The 20% top overlap maps are shown in Figures 4 and 5. It is important to note that the areas that are not colored in signify the absence of any consistency regarding the nodes in that anatomical space. Additionally, the scale values on the overlap images are indicative of the percentage of within-group consistency. The scales were bounded on a per-image basis, so as to maximize the number of high consistency areas shown. Based on visual inspections of the images, it appears that the consistency of top percentage nodes is more concentrated in the subcortical areas in the Parkinson's group when compared to the controls: in Figures 4 and 5 the subcortical regions (thalamus, caudate, etc.) have higher E_{glob} consistency (~15%-20% vs. about ~0-10%), and higher E_{loc} consistency (~15%-40% vs. ~10%-20% with one 40% area).

Although testing this hypothesis statistically is beyond the scope of the current study, these images nevertheless help to illustrate the differences in the consistency between top percentage nodes between groups.

The highest concentration of E_{glob} consistencies in the Parkinson's group are located in the left precentral gyrus, left rolandic operculum, and the left inferior frontal gyrus (all about 50% consistent). The subcortical areas are represented, but they are not the most consistent (e.g., the thalamus is about 10% consistent). Additional disease-relevant high consistency areas include the left insula and left cingulate gyrus (about 40%). High consistency E_{loc} areas in the Parkinson's group also include the left heschl gyrus, left temporal gyrus (50%) right thalamus, left cuneus, and the left gyrus rectus (40%).

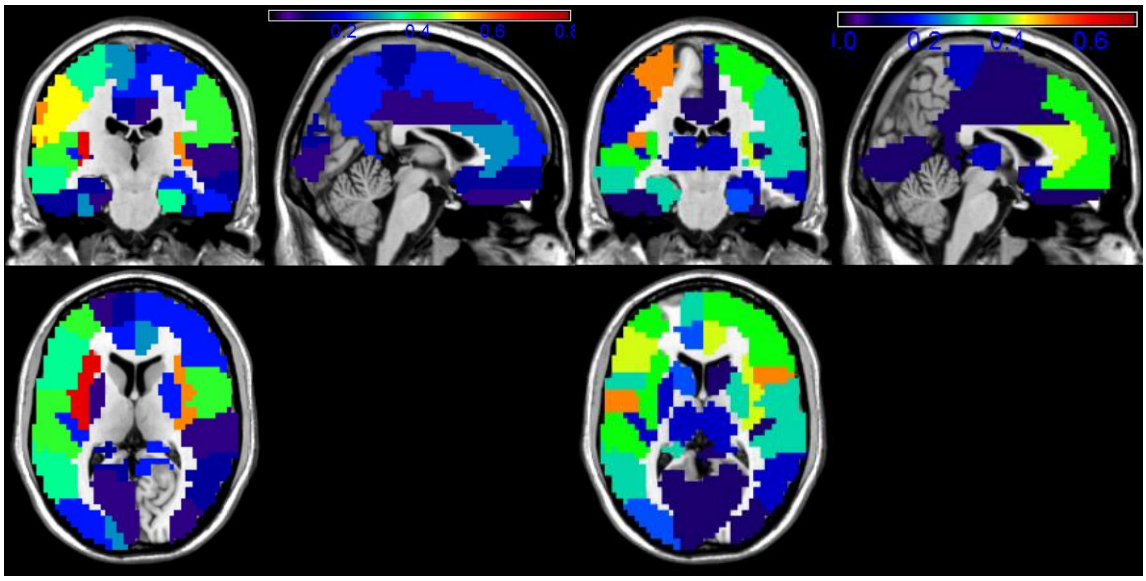

Figure 4. E_{glob} top overlap map for controls (left) and Parkinson's (right). The control map is bounded from 0%-80%, and the Parkinson's image is bounded form 0-70%.

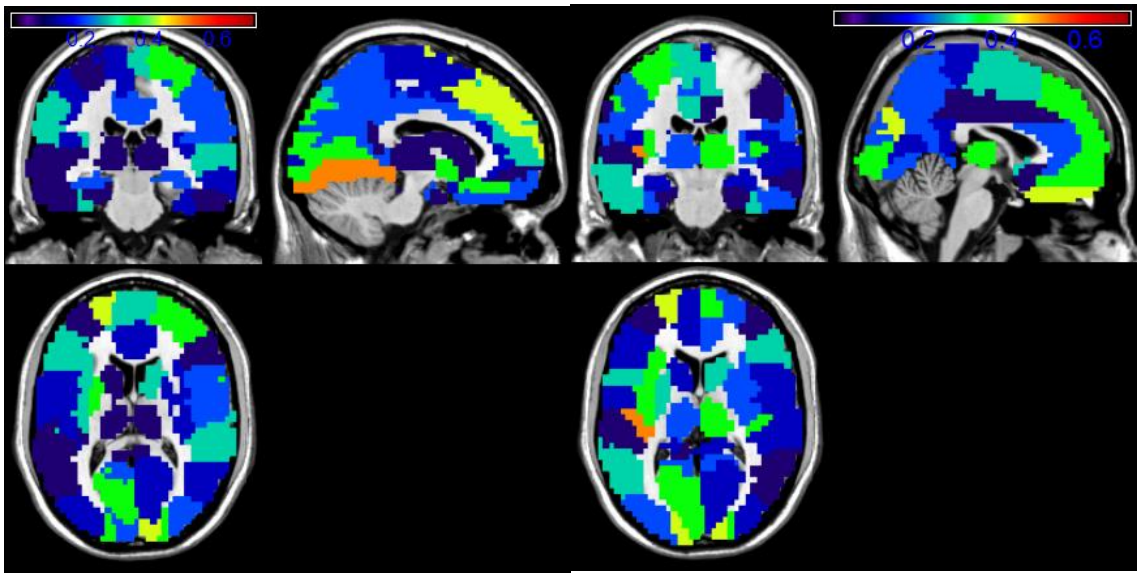

Figure 5. E_{loc} top overlap map for controls (left) and Parkinson's (right), both bounded from 0% to 70%.

In the control E_{glob} overlap, the highest percentage consistency areas included the left insula (80%), right insula, left postcentral gyrus and the inferior parietal lobule

(50%). Furthermore, in the control E_{loc} overlap, the highest consistency nodes were the left lingual gyrus (50%), right cuneus (~45%), the left superior parietal gyrus, left middle frontal gyrus and right superior temporal gyrus (~40%).

Subcortical Module Membership Permutation Test

In order to test for disease-related differences in modularity, a permutation procedure was run to compare the modular membership of subcortical nodes. Significant results would mean that the members of the given subcortical node's module are different between groups, suggesting that modular organization at-rest is different between patients and controls. The results of the permutation procedure revealed no significant between-group differences in the subcortical nodes' modules, using an FDR correction rate of 5%. Before the correction for multiple comparisons, the Left Thalamus's module membership was found to be significantly different between groups ($p < .05$). From a purely exploratory viewpoint, the module contents of the Left Thalamus appear to vary greatly between groups. Because the thalamus appears to be a significant contributor to the relationship between subcortical efficiency and behavioral outcomes, Appendix A presents the module contents for the Left Thalamus in each group.

From an exploratory standpoint, the Left Thalamus's modular contents appear to be highly integrative across the brain in Parkinson's when compared to the controls. In order to test this assumption, the number of nodes in each module that contained the Left Thalamus was calculated, and a t-test was performed between groups in order to ascertain if one group had, on average, more nodes in modules that also contained the Left Thalamus. The t-test revealed that the Parkinson's group had significantly more members in modules that contained the Left Thalamus than the control group, $t(26) = 2.51$, $d = .98$,

$p < .05$. Although this does not statistically demonstrate a difference in the members of the module, it does show that the "Left Thalamus module" is more integrative of additional areas than in controls. This idea is supported by the evidence presented earlier regarding supplementary, compensatory connections in Parkinson's that do not exist in controls, and the significant between-groups difference in left and right thalamic E_{loc}.

Differences in Q

There was no significant between-group difference in *Q*, $t(26) = 1.647$, $d = .65$, $p > .05$. Inconsistent with our hypotheses, *Q* also failed to significantly correlate with any of the behavioral and clinical outcomes in the Parkinson's group ($p > .05$). This may be due to the normalizing effects of levodopa on the Parkinson's patients' networks, as it reduces the need for compensatory connections across modules.

Differences in Module Counts

A t-test revealed no significant differences in the number of modules between groups, $t(26) = -.526$, $d = -.20$, $p > .05$. Additionally, the number of modules did not significantly correlate with any of the behavioral and clinical measures in the Parkinson's group ($p > .05$ **).**

DISCUSSION

The primary aim of this study was to examine differences in resting-state network subcortical efficiency and modular construction between patients with Parkinson's disease and healthy controls. Specifically, this study sought to assess how potential network biomarkers of pathology and subcortical efficiency profiles were expressed in Parkinson's patients that were in the "ON" state of their medication.

Despite the apparent normalizing effects of levodopa, subcortical efficiency in Parkinson's was tied to the clinical severity of several nonmotor symptoms as indicated by the correlations between subcortical global and local efficiency and the collected clinical measures (see Table 10). The thalamus, caudate, and pallidum were the specific subcortical nodes that seemed to be driving these effects: These nodes were all significantly higher in either E_{glob} (left caudate and left pallidum) or E_{loc} (left and right thalamus) in the Parkinson's group compared to controls. The relationship between these particular nodes and behavioral deficits makes sense since these areas are also relevant to disease pathology: the globus pallidus is anatomically subsumed by the pallidum node and the striatum by the caudate node

Currently, there is no comparable study in the Parkinson's functional connectivity literature to directly compare the clinical and behavioral findings to. Functional connectivity studies of Parkinson's disease have not examined global and local efficiency in this context before. This leaves the interpretation of these findings to be somewhat open. One hypothesis is that the subcortical nodes are driving these relationships via compensatory functional connections received from the cortex.

The compensation hypothesis is supported by evidence showing that cortical links that are high in anatomical distance may be broadly related to neural dysfunction. In a study about how the anatomical distance of nodal connections influences network construction in schizophrenia, Alexander-Bloch and colleagues (2013) found that increased anatomical distance between connected nodes in those with schizophrenia was associated with reduced clustering and modularity, a stronger symptomatic burden, and increased global efficiency.

From a network science perspective, it could be argued that high anatomical connection distance may be directly related to higher global efficiency, as the number of jumps necessary to reach disparate regions of the brain should decrease as a function of global efficiency increasing. Thus, a higher global efficiency score for any given area could be indicative of higher anatomical distance subsumed by that area. With increasing global efficiency, a node is either becoming more like a hub of connections or it is becoming more connected to an already established hub. Given the evidence for higher E_{glob} in the left pallidum and left caudate in the Parkinson's group, it could be the case that these two nodes have long-distance anatomical connections as a function of being linked to strongly connected cortical areas that then lead to higher nodal E_{glob}.

As mentioned previously, the left and right thalamic nodes had significantly higher nodal E_{loc} in the Parkinson's group. Because local efficiency is determined by N^{th} order connections, and not a node's immediate connections, it is more difficult to assert that these differences are evidence of long-range connections. It may be the case that the thalamic nodes are linked to a well-connected cluster of nodes in an anatomically proximal region of the brain, or to a similar cluster in a distal region of the brain. Further

inquiry into the connectivity profile of the thalamic nodes using standardized brain spaces would give a definitive answer to the existence of long-range connections from the thalamic nodes, but this extends beyond the scope of the current study.

Recent research has demonstrated that local efficiency scores in the limbic system (using the thalamus and hippocampus) effectively discriminate between Parkinson's patients "OFF" medicine and controls with lower efficiency, in Parkinson's (Zhang et al., 2014). The results from the current "ON" medication study show a reversal of this result, insofar as Thalamic E_{loc} was significantly higher in the Parkinson's group, and might be discriminating patients from controls in the opposite fashion. The reversal of these findings in the current study show that the limbic system, specifically the thalamus, may be key to finding a discriminatory biomarker that seems to be reversed entirely by the administration of levodopa. Additional, larger follow-up studies with patients in the "ON" state with the same methods used by Zhang and colleagues (2014) would help confirm this hypothesis.

One of the main differences between the present study and the current functional connectivity literature on Parkinson's disease is the usage of patients in the "ON" medicine state. As such, this decision has implications for a variety of our findings. As hypothesized, levodopa had several normalizing effects on the Parkinsonian networks. Consistent with the findings in Achard and Bullmore (2007), whole-brain global and local efficiency measures for the Parkinson's group were found to not differ from controls. Additionally, there were no significant between-group differences in the number of modules or the composition of the subcortical modules.

It is unclear as to whether this is a consequence of a low sample size, the normalization effects of levodopa, or the absence of any true difference in subcortical module members. Given that the Left Thalamus node was found to significantly differ before the correction for multiple comparisons, with several other nodes also approaching significance, it may be that the study was too underpowered to find actual differences. This idea is validated by (a) the qualitative examination of the members of the Left Thalamus module between groups (see Appendix A), (b) the significant between-group difference in the number of nodes in each module that contains the Left Thalamus., and (c) the nodal-level differences in Left and Right Thalamic E_{loc}. Exploration of the composition of subcortical nodes in Parkinson's patients who were "OFF" medication would be an interesting follow-up experiment.

The consistency of high global and local efficiency nodes was also revealing. The overlap images provided an exploratory look into the consistency of key nodes in the Parkinson's group and controls. The top highest consistency areas across all participants included nodes that are part of, or at least connected to, default and executive mode network areas such as the precentral gyrus, temporal gyrus, and cuneus (Uddin et al., 2009).

One of the highest consistency E_{glob} nodes in both groups was the left insular cortex, or simply the left insula (~40% in Parkinson's, ~70% controls). The insula has been implicated as being critical to the expression of nonmotor symptoms of Parkinson's disease, while also simultaneously being extremely under-studied in the literature (Christopher et al., 2014). It is also related to a number of the collected behavioral measures: the anterior insula is a key region involved in the experience of empathy, and

may be responsible for the expression of apathy and depression in Parkinson's (Leigh et al., 2013). Furthermore, reduced functional connectivity of the insula has been directly related to poor impulse control and gambling disorders in Parkinson's (Cilia et al., 2011).

Therefore, because the insula was one of the highest in consistency of E_{glob} nodes in both groups it may be the case that there is a mechanism of compensation acting on the insula when patients are in the "ON" medicine state that brings their consistency scores closer to controls. As "OFF" medication findings have shown the insula to be less connected, this discovery highlights the importance of further studying the connectivity of the insula in Parkinson's (Christopher et al., 2014).

Another one of the highest consistency E_{glob} nodes that is relevant to Parkinson's disease pathology was the left anterior cingulate gyrus (~40%). The anterior cingulate has been heavily implicated in reward processing disturbances in Parkinson's disease, and dopaminergic dysfunction in this area has been related to the heightened expression of impulsive behaviors in the disease (Rowe et al., 2008). Further analysis into the cingulate gyrus's connectivity profile could elaborate on how this efficiency is expressed in its relationship to patients' impulsivity scores.

As mentioned earlier, the left heschl gyrus (~50%) was the highest in E_{loc} consistency in the Parkinson's group. This finding is a reversal of previous research that has found the heschl gyri to be significantly lower in local efficiency in Parkinson's patients that were "OFF" medicine (Zhang et al., 2014). This finding is confirmed by evidence that shows late-stage Parkinson's disease, as measured by the Braak staging method, as being partly characterized by destruction of areas around and inside the heschl (Braak et al., 2003). Thus, it may be the case that there is either another mechanism of

compensation, like the insula, or normalizing effects from levodopa that is creating these results in the "ON" state.

Additionally, the right thalamus, and to a lesser degree the left thalamus, was also a top consistency (~40%) E_{loc} node in the Parkinson's group. Coupled with the already discussed results regarding the thalamus's involvement in possible compensatory mechanisms, the overlap maps provide a further impetus for the investigation of any differences in its connectivity profile in both the "ON" and "OFF" states.

Limitations and Future Directions

One of the main limitations of the current study is its relatively small sample size. Functional connectivity studies of diseased brains have been conducted with similarly sized groups before (e.g., Gorges et al., 2015; Hacker et al., 2012; Skidmore et al., 2014; Yao et al., 2014), but it nevertheless puts a hard limit on statistical power. For example, a larger sample size would increase the power of the FDR correction, and also of the permutation test itself. A second major limitation was the absence of behavioral data for the control group. Investigating the relationship of subcortical and cortical efficiencies to the impulsivity, depression, and cognitive functioning in controls would help elucidate the findings regarding these relationships in Parkinson's patients. A third major limitation is the possibility that some of the significant correlations are Type I errors because of the number of comparisons that were run.

The last important limitation of this study is that patients' data were available only in the "ON" state of medication. This did allow for comparisons to similar studies that had patients in the "ON" state (e.g., Wei et al., 2014), but also sacrificed the ability to do repeated measures investigations of the Parkinson's group. Future studies using

both “ON” and “OFF” state scans for the same group of participants would shed new light on the effects of levodopa and the existence of the current study’s results in the “OFF” state. Novel repeated measures investigations could include examining medication state differences in subcortical efficiency relationships, *Q* values, behavioral scores, nodal-level efficiencies, and subcortical modular membership.

Lastly, given the results found regarding differences in thalamic efficiency, future studies should analyze the efficiencies of the thalamus and other parts of the limbic system, as they seem to play a significant role in differentiating Parkinson’s patients from controls, regardless of medicine state. A repeated-measures investigation into how limbic efficiency changes from “ON” to “OFF” would also help in understanding how and what additional areas may change.

Conclusion

Palop, Chin, and Mucke (2006) propose that the fluctuations in day-to-day functioning of those with neurodegenerative disorders cannot entirely be represented by neuronal loss, and that variations in functional network connections can instead better inform us. The present study is consistent with this in that it suggests differences in functional connectivity in Parkinson’s disease can provide useful information in characterizing disease pathology. In particular, global and local efficiencies of the subcortical regions and the limbic system were tied to behavioral and clinical outcomes. These relationships did not exist on a whole-brain level. Further exploration into the network properties of the subcortical regions in Parkinson’s disease may yield additional insight into the integral role that they play in disease pathology.

REFERENCES

Achard, S., & Bullmore, E. (2007). Efficiency and cost of economical brain functional networks. *PLoS Comput Biol*, *3*(2), e17.

Achard, S., Salvador, R., Whitcher, B., Suckling, J., & Bullmore, E. D. (2006). A resilient, low-frequency, small-world human brain functional network with highly connected association cortical hubs. *The Journal of Neuroscience*, *26*(1), 63-72.

Ajilore, O., Lamar, M., & Kumar, A. (2014). Association of brain network efficiency with aging, depression, and cognition. *The American Journal of Geriatric Psychiatry*, *22*(2), 102-110.

Alexander-Bloch, A. F., Vértes, P. E., Stidd, R., Lalonde, F., Clasen, L., Rapoport, J., & Gogtay, N. (2012). The anatomical distance of functional connections predicts brain network topology in health and schizophrenia. *Cerebral cortex*, bhr388.

Alexander-Bloch, A., Lambiotte, R., Roberts, B., Giedd, J., Gogtay, N., & Bullmore, E. (2012). The discovery of population differences in network community structure: new methods and applications to brain functional networks in schizophrenia. *Neuroimage*, *59*(4), 3889-3900.

Beyer, M. K., Janvin, C. C., Larsen, J. P., & Aarsland, D. (2007). A magnetic resonance imaging study of patients with Parkinson's disease with mild cognitive impairment and dementia using voxel-based morphometry. *Journal of Neurology, Neurosurgery & Psychiatry*, *78*(3), 254-259.

Bonneville, F., Welter, M. L., Elie, C., du Montcel, S. T., Hasboun, D., Menuel, C., & Navarro, S. (2005). Parkinson disease, brain volumes, and subthalamic nucleus stimulation. *Neurology*, *64*(9), 1598-1604.

Braak, H., Del Tredici, K., Rüb, U., de Vos, R. A., Steur, E. N. J., & Braak, E. (2003). Staging of brain pathology related to sporadic Parkinson's disease. *Neurobiology of Aging*, *24*(2), 197-211.

Bullmore, E., & Sporns, O. (2009). Complex brain networks: graph theoretical analysis of structural and functional systems. *Nature Reviews Neuroscience*, *10*(3), 186-198.

Chau, W., & McIntosh, A. R. (2005). The Talairach coordinate of a point in the MNI space: How to interpret it. *Neuroimage*, *25*(2), 408-416.

Chaudhuri, K. R., Healy, D. G., & Schapira, A. H. (2006). Non-motor symptoms of Parkinson's disease: Diagnosis and management. *The Lancet Neurology*, *5*(3), 235-245.

Christopher, L., Koshimori, Y., Lang, A. E., Criaud, M., & Strafella, A. P. (2014). Uncovering the role of the insula in non-motor symptoms of Parkinson's disease. *Brain*, *137*(8), 2143-2154.

Cilia, R., & van Eimeren, T. (2011). Impulse control disorders in Parkinson's disease: Seeking a roadmap toward a better understanding. *Brain Structure and Function*, *216*(4), 289-299.

Davie, C. A. (2008). A review of Parkinson's disease. *British Medical Bulletin*, *86*(1), 109-127.

DeLong, M., & Wichmann, T. (2010). Changing views of basal ganglia circuits and circuit disorders. *Clinical EEG and neuroscience*, *41*(2), 61-67.

Dickerson, B. C., Stoub, T. R., Shah, R. C., Sperling, R. A., Killiany, R. J., Albert, M. S., & Blacker, D. (2011). Alzheimer-signature MRI biomarker predicts AD dementia in cognitively normal adults. *Neurology*, *76*(16), 1395-1402.

Dubbelink, K. T. O., Hillebrand, A., Stoffers, D., Deijen, J. B., Twisk, J. W., Stam, C. J., & Berendse, H. W. (2013). Disrupted brain network topology in Parkinson's disease: A longitudinal magnetoencephalography study. *Brain*, awt316.

Eguiluz, V. M., Chialvo, D. R., Cecchi, G. A., Baliki, M., & Apkarian, A. V. (2005). Scale-free brain functional networks. *Physical Review Letters*, *94*(1), 018102.

Feldmann, A., Illes, Z., Kosztolanyi, P., Illes, E., Mike, A., Kover, F., & Nagy, F. (2008). Morphometric changes of gray matter in Parkinson's disease with depression: A voxel-based morphometry study. *Movement Disorders*, *23*(1), 42-46.

Fernandez, H. H. (2015). 2015 Update on Parkinson disease. *Cleveland Clinical Journal of Medicine*, *82*(9):563-8. doi: 10.3949/ccjm.82gr.15004.

Fischl, B., Rajendran, N., Busa, E., Augustinack, J., Hinds, O., Yeo, B. T., & Zilles, K. (2008). Cortical folding patterns and predicting cytoarchitecture. *Cerebral Cortex*, *18*(8), 1973-1980.

Gorges, M., Müller, H. P., Lulé, D., Pinkhardt, E. H., Ludolph, A. C., Kassubek, J., & LANDSCAPE Consortium. (2015). To rise and to fall: Functional connectivity in cognitively normal and cognitively impaired patients with Parkinson's disease. Nambu, A. (2011). Somatotopic organization of the primate basal ganglia. *Frontiers in neuroanatomy*, *5*, 26.

Göttlich, M., Münte, T. F., Heldmann, M., Kasten, M., Hagenah, J., & Krämer, U. M. (2013). Altered resting state brain networks in Parkinson's disease.

Greicius, M. (2008). Resting-state functional connectivity in neuropsychiatric disorders. *Current opinion in neurology*, *21*(4), 424-430.

Grinberg, L. T., Rueb, U., di Lorenzo Alho, A. T., & Heinsen, H. (2010). Brainstem pathology and non-motor symptoms in PD. *Journal of the Neurological Sciences*, *289*(1), 81-88.

Hacker, C., Perlmutter, J., Criswell, S., Ances, B., & Snyder, A. (2012). Resting state functional connectivity of the striatum in Parkinson's disease. *Brain*, aws281.

He, J. H., Cui, Y., Song, M., Yang, Y., Dang, Y. Y., Jiang, T. Z., & Xu, R. X. (2015). Decreased functional connectivity between the mediodorsal thalamus and default mode network in patients with disorders of consciousness. *Acta Neurologica Scandinavica*, *131*(3), 145-151.

Helmich, R. C., Derikx, L. C., Bakker, M., Scheeringa, R., Bloem, B. R., & Toni, I. (2010). Spatial remapping of cortico-striatal connectivity in Parkinson's disease. *Cerebral Cortex*, *20*(5), 1175-1186.

Ibarretxe-Bilbao, N., Junque, C., Segura, B., Baggio, H. C., Marti, M. J., Valldeoriola, F., & Tolosa, E. (2012). Progression of cortical thinning in early Parkinson's disease. *Movement Disorders*, *27*(14), 1746-1753.

Jankovic, J. (2008). Parkinson's disease: clinical features and diagnosis. *Journal of Neurology, Neurosurgery & Psychiatry*, *79*(4), 368-376.

Khazaee, A., Ebrahimzadeh, A., & Babajani-Feremi, A. (2015). Identifying patients with Alzheimer's disease using resting-state fMRI and graph theory. *Clinical Neurophysiology*, *126*(11), 2132-2141.

Knierim, J. (2016). Basal Ganglia (Section 3, Chapter 4) Neuroscience Online: An Electronic Textbook for the Neurosciences | Department of Neurobiology and Anatomy - The University of Texas Medical School at Houston. Retrieved March 02, 2016, from http://neuroscience.uth.tmc.edu/s3/chapter04.html

Labrenz, F., Wrede, K., Forsting, M., Engler, H., Schedlowski, M., Elsenbruch, S., & Benson, S. (2015). Alterations in functional connectivity of resting state networks during experimental endotoxemia–An exploratory study in healthy men. *Brain, Behavior, and Immunity*, 54, 17-26.

Lang, A. E., & Lozano, A. M. (1998). Parkinson's disease. *New England Journal of Medicine*, *339*(15), 1044-1053.

Latora, V., & Marchiori, M. (2001). Efficient behavior of small-world networks. *Physical review letters*, *87*(19), 198701.

Lebedev, A. V., Westman, E., Simmons, A., Lebedeva, A., Siepel, F. J., Pereira, J. B., & Aarsland, D. (2014). Large-scale resting state network correlates of cognitive impairment in Parkinson's disease and related dopaminergic deficits. *Frontiers in Systems Neuroscience*, *8*, 45. doi: 10.3389/fnsys.2014.00045

Lee, T. K., Chau, R., & Leong, S. K. (1995). The anatomy of the basal ganglia and Parkinson's disease: A review. *Singapore Medical Journal*, *36*(1), 74-76.

Lee, V. M. Y., & Trojanowski, J. Q. (2006). Mechanisms of Parkinson's disease linked to pathological α-synuclein: New targets for drug discovery. *Neuron*, *52*(1), 33-38.

Leigh, R., Oishi, K., Hsu, J., Lindquist, M., Gottesman, R. F., Jarso, S., & Hillis, A. E. (2013). Acute lesions that impair affective empathy. *Brain*, *136*(8), 2539-2549.

Luo, C., Song, W., Chen, Q., Zheng, Z., Chen, K., Cao, B., & Shang, H. F. (2014). Reduced functional connectivity in early-stage drug-naive Parkinson's disease: A resting-state fMRI study. *Neurobiology of Aging*, *35*(2), 431-441.

Magalhães, R., Marques, P., Soares, J., Alves, V., & Sousa, N. (2015). The impact of normalization and segmentation on resting-state brain networks. *Brain Connectivity*, *5*(3), 166-176.

Maidan, I., Rosenberg-Katz, K., Jacob, Y., Giladi, N., Deutsch, J. E., Hausdorff, J. M., & Mirelman, A. (2016). Altered brain activation in complex walking conditions in patients with Parkinson's disease. *Parkinsonism & Related Disorders*, *25*, 91-96.

Newman, M. E., & Girvan, M. (2004). Finding and evaluating community structure in networks. *Physical Review E*, *69*(2), 026113.

Onoda, K., & Yamaguchi, S. (2013). Small-worldness and modularity of the resting-state functional brain network decrease with aging. *Neuroscience letters*, *556*, 104-108.

Pahapill, P. A., & Lozano, A. M. (2000). The pedunculopontine nucleus and Parkinson's disease. *Brain*, *123*(9), 1767-1783.

Palop, J. J., Chin, J., & Mucke, L. (2006). A network dysfunction perspective on neurodegenerative diseases. *Nature*, *443*(7113), 768-773.

Paulsen, J. S., Zimbelman, J. L., Hinton, S. C., Langbehn, D. R., Leveroni, C. L., Benjamin, M. L., & Rao, S. M. (2004). fMRI biomarker of early neuronal dysfunction in presymptomatic Huntington's disease. *American Journal of Neuroradiology*, *25*(10), 1715-1721.

Pellicano, C., Benincasa, D., Pisani, V., Buttarelli, F. R., Giovannelli, M., & Pontieri, F. E. (2007). Prodromal non-motor symptoms of Parkinson's disease. *Neuropsychiatric Disease and Treatment, 3*(1), 145–152.

Power, J. D., Barnes, K. A., Snyder, A. Z., Schlaggar, B. L., & Petersen, S. E. (2012). Spurious but systematic correlations in functional connectivity MRI networks arise from subject motion. *Neuroimage, 59*(3), 2142-2154.

Pyatigorskaya, N., Gallea, C., Garcia-Lorenzo, D., Vidailhet, M., & Lehericy, S. (2014). A review of the use of magnetic resonance imaging in Parkinson's disease. *Therapeutic Advances in Neurological Disorders, 7*(4), 206–220. http://doi.org/10.1177/1756285613511507

Rosenberg, M. D., Finn, E. S., Scheinost, D., Papademetris, X., Shen, X., Constable, R. T., & Chun, M. M. (2015). A neuromarker of sustained attention from whole-brain functional connectivity. *Nature neuroscience, 19*, 165-171.

Rowe, J. B., Hughes, L., Ghosh, B. C. P., Eckstein, D., Williams-Gray, C. H., Fallon, S., & Owen, A. M. (2008). Parkinson's disease and dopaminergic therapy—differential effects on movement, reward and cognition. *Brain, 131*(8), 2094-2105.

Rubinov, M., & Sporns, O. (2010). Complex network measures of brain connectivity: Uses and interpretations. *Neuroimage*, *52*(3), 1059-1069.

Schwarz, A. J., & McGonigle, J. (2011). Negative edges and soft thresholding in complex network analysis of resting state functional connectivity data. *Neuroimage, 55*(3), 1132-1146.

Schwarz, A. J., & McGonigle, J. (2011). Negative edges and soft thresholding in complex network analysis of resting state functional connectivity data. *Neuroimage, 55*(3), 1132-1146.

Seibert, T. M., & Brewer, J. B. (2011). Default network correlations analyzed on native surfaces. *Journal of Neuroscience Methods*, *198*(2), 301-311.

Seibert, T. M., Murphy, E. A., Kaestner, E. J., & Brewer, J. B. (2012). Interregional correlations in Parkinson disease and Parkinson-related dementia with resting functional MR imaging. *Radiology, 263*(1), 226-234.

Simpson, S. L., Bowman, F. D., & Laurienti, P. J. (2013). Analyzing complex functional brain networks: fusing statistics and network science to understand the brain. *Statistics Surveys*, *7*, 1.

Skidmore, F., Korenkevych, D., Liu, Y., He, G., Bullmore, E., & Pardalos, P. M. (2011). Connectivity brain networks based on wavelet correlation analysis in Parkinson fMRI data. *Neuroscience Letters, 499*(1), 47-51.

Tessitore, A., Giordano, A., Russo, A., & Tedeschi, G. (2015). Structural connectivity in Parkinson's disease. *Parkinsonism and Related Disorders,22*(1), S56-S59.

Tzourio-Mazoyer, N., Landeau, B., Papathanassiou, D., Crivello, F., Etard, O., Delcroix, N., & Joliot, M. (2002). Automated anatomical labeling of activations in SPM using a macroscopic anatomical parcellation of the MNI MRI single-subject brain. *Neuroimage*, *15*(1), 273-289.

Uddin, L. Q., Clare Kelly, A. M., Biswal, B. B., Xavier Castellanos, F., & Milham, M. P. (2009). Functional connectivity of default mode network components: Correlation, anticorrelation, and causality. *Human Brain Mapping*, *30*(2), 625-637.

Vervoort, G., Alaerts, K., Bengevoord, A., Nackaerts, E., Heremans, E., Vandenberghe, W., & Nieuwboer, A. (2016). Functional connectivity alterations in the motor and fronto-parietal network relate to behavioral heterogeneity in Parkinson's disease. *Parkinsonism & Related Disorders*, *24*, 48-55.

Wang, J. H., Zuo, X. N., Gohel, S., Milham, M. P., Biswal, B. B., & He, Y. (2011). Graph theoretical analysis of functional brain networks: Test-retest evaluation on short-and long-term resting-state functional MRI data. *PloS one*, *6*(7), e21976.

Wei, L., Zhang, J., Long, Z., Wu, G. R., Hu, X., Zhang, Y., & Wang, J. (2014). Reduced topological efficiency in cortical-basal Ganglia motor network of Parkinson's disease: A resting state fMRI study. *PloS one*, *9*(10), e108124.

Wu, T., Wang, L., Chen, Y., Zhao, C., Li, K., & Chan, P. (2009). Changes of functional connectivity of the motor network in the resting state in Parkinson's disease. *Neuroscience Letters*, *460*(1), 6-10.

Zalesky, A., Fornito, A., Harding, I. H., Cocchi, L., Yücel, M., Pantelis, C., & Bullmore, E. T. (2010). Whole-brain anatomical networks: Does the choice of nodes matter?. *Neuroimage*, *50*(3), 970-983.

Zhang, D., Liu, X., Chen, J., & Liu, B. (2014). Distinguishing patients with Parkinson's disease subtypes from normal controls based on functional network regional efficiencies. *PloS one*, *9*(12), e115131.

Zhang, D., Wang, J., Liu, X., Chen, J., & Liu, B. (2015). Aberrant brain network efficiency in Parkinson's disease patients with tremor: A multi-modality study. *Frontiers in aging neuroscience*, *7*, 169.

APPENDIX A

8	9	10	11	12	13	14
Precentral_R	Insula_L	Cingulum_Post_L	Hippocampus_R	Thalamus_L	Frontal_Sup_L	Olfactory_L
Postcentral_R	Insula_R	Cingulum_Post_R	ParaHippocampal_L	Thalamus_R	Frontal_Sup_R	Hippocampus_L
Parietal_Sup_R	Hippocampus_L	Fusiform_L	ParaHippocampal_R	Temporal_Pole_Mid_L	Frontal_Sup_Medial_L	Hippocampus_R
Putamen_L	Hippocampus_R	Fusiform_R	Thalamus_L	Temporal_Pole_Mid_R	Frontal_Sup_Medial_R	ParaHippocampal_R
Pallidum_L	ParaHippocampal_R	Thalamus_L	Thalamus_R		Cingulum_Ant_R	Caudate_L
Pallidum_R	Amygdala_L	Thalamus_R			Cingulum_Mid_L	Caudate_R
Thalamus_L	Amygdala_R	Temporal_Sup_L			Cingulum_Mid_R	Putamen_L
	Fusiform_L	Temporal_Sup_R			Caudate_R	Putamen_R
	Fusiform_R	Temporal_Mid_L			Thalamus_L	Pallidum_L
	Putamen_L	Temporal_Mid_R				Pallidum_R
	Putamen_R	Temporal_Pole_Mid_L				Thalamus_L
	Pallidum_L	Temporal_Pole_Mid_R				Thalamus_R
	Pallidum_R	Temporal_Inf_L				Heschl_L
	Thalamus_L	Temporal_Inf_R				
	Thalamus_R					
	Heschl_L					
	Temporal_Sup_L					
	Temporal_Pole_Sup_L					
	Temporal_Pole_Mid_L					

1	2	3	4	5	6	7
ParaHippocampal_L	Thalamus_L	Frontal_Inf_Tri_L	Frontal_Inf_Orb_L	Fusiform_R	Rolandic_Oper_R	Olfactory_L
ParaHippocampal_R		Hippocampus_R	Rolandic_Oper_L	Caudate_L	Postcentral_R	Olfactory_R
Amygdala_L		ParaHippocampal_R	Insula_L	Caudate_R	SupraMarginal_L	Hippocampus_L
Amygdala_R		Amygdala_R	Calcarine_L	Thalamus_L	Thalamus_L	Hippocampus_R
Fusiform_L		Cuneus_L	Lingual_L	Thalamus_R	Thalamus_R	ParaHippocampal_L
Fusiform_R		Pallidum_L	Occipital_Mid_L		Heschl_L	ParaHippocampal_R
Caudate_L		Thalamus_L	Occipital_Inf_R		Heschl_R	Amygdala_R
Caudate_R		Heschl_R	Caudate_L		Temporal_Sup_L	Occipital_Mid_R
Thalamus_L		Temporal_Sup_R	Putamen_L		Temporal_Sup_R	Fusiform_R
Thalamus_R		Temporal_Mid_R	Pallidum_L		Temporal_Mid_L	Caudate_L
Heschl_L		Temporal_Pole_Mid_R	Thalamus_L		Temporal_Mid_R	Putamen_L
Temporal_Pole_Mid_L		Temporal_Inf_L			Temporal_Inf_L	Putamen_R
Temporal_Pole_Mid_R		Temporal_Inf_R			Temporal_Inf_R	Pallidum_L
Temporal_Inf_L						Pallidum_R
						Thalamus_L
						Heschl_L

Nodal membership for the Left Thalamus module. Parkinson's group.

1	2	3	4	5	6	7
Caudate_R	Thalamus_L	Caudate_R	Thalamus_L	Precentral_L	Caudate_L	Thalamus_L
Thalamus_L	Thalamus_R	Putamen_L	Thalamus_R	Frontal_Sup_L	Thalamus_L	
Thalamus_R		Thalamus_L		Frontal_Mid_L	Thalamus_R	
		Thalamus_R		Frontal_Mid_Orb_L		
				Frontal_Inf_Oper_L		
				Frontal_Inf_Tri_L		
				Frontal_Inf_Orb_L		
				Rolandic_Oper_L		
				Thalamus_L		
				Heschl_L		
				Temporal_Sup_L		
				Temporal_Sup_R		
				Temporal_Mid_L		

8	9	10	11	12	13	14
Thalamus_L	Precentral_R	Hippocampus_L	Hippocampus_L	Thalamus_L	Amygdala_L	Thalamus_L
	Cingulum_Post_L	Hippocampus_R	Hippocampus_R	Thalamus_R	Thalamus_L	
	Postcentral_L	ParaHippocampal_L	ParaHippocampal_L		Thalamus_R	
	Postcentral_R	ParaHippocampal_R	Amygdala_L			
	Parietal_Sup_L	Amygdala_L	Amygdala_R			
	Parietal_Sup_R	Amygdala_R	Fusiform_L			
	Parietal_Inf_L	Thalamus_L	Caudate_L			
	Parietal_Inf_R	Thalamus_R	Putamen_L			
	SupraMarginal_L	Temporal_Pole_Mid_R	Putamen_R			
	SupraMarginal_R		Pallidum_L			
	Precuneus_L		Pallidum_R			
	Paracentral_Lobule_L		Thalamus_L			
	Caudate_L		Thalamus_R			
	Thalamus_L		Temporal_Inf_R			
	Thalamus_R					
	Heschl_L					

Nodal membership for the Left Thalamus module. Control group.

APPENDIX B

List of AAL Nodes Used

	Label
1	Precentral_L
2	Precentral_R
3	Frontal_Sup_L
4	Frontal_Sup_R
5	Frontal_Sup_Orb_L
6	Frontal_Sup_Orb_R
7	Frontal_Mid_L
8	Frontal_Mid_R
9	Frontal_Mid_Orb_L
10	Frontal_Mid_Orb_R
11	Frontal_Inf_Oper_L
12	Frontal_Inf_Oper_R
13	Frontal_Inf_Tri_L
14	Frontal_Inf_Tri_R
15	Frontal_Inf_Orb_L
16	Frontal_Inf_Orb_R
17	Rolandic_Oper_L
18	Rolandic_Oper_R
19	Supp_Motor_Area_L
20	Supp_Motor_Area_R
21	Olfactory_L
22	Olfactory_R
23	Frontal_Sup_Medial_L
24	Frontal_Sup_Medial_R
25	Frontal_Med_Orb_L
26	Frontal_Med_Orb_R
27	Rectus_L
28	Rectus_R
29	Insula_L
30	Insula_R
31	Cingulum_Ant_L
32	Cingulum_Ant_R
33	Cingulum_Mid_L
34	Cingulum_Mid_R
35	Cingulum_Post_L
36	Cingulum_Post_R
37	Hippocampus_L
38	Hippocampus_R
39	ParaHippocampal_L
40	ParaHippocampal_R
41	Amygdala_L
42	Amygdala_R
43	Calcarine_L
44	Calcarine_R
45	Cuneus_L
46	Cuneus_R
47	Lingual_L
48	Lingual_R
49	Occipital_Sup_L
50	Occipital_Sup_R
51	Occipital_Mid_L
52	Occipital_Mid_R
53	Occipital_Inf_L
54	Occipital_Inf_R
55	Fusiform_L
56	Fusiform_R
57	Postcentral_L
58	Postcentral_R
59	Parietal_Sup_L
60	Parietal_Sup_R
61	Parietal_Inf_L
62	Parietal_Inf_R
63	SupraMarginal_L
64	SupraMarginal_R
65	Angular_L
66	Angular_R
67	Precuneus_L
68	Precuneus_R
69	Paracentral_Lobule_L
70	Paracentral_Lobule_R
71	Caudate_L
72	Caudate_R
73	Putamen_L
74	Putamen_R

75 Pallidum_L
76 Pallidum_R
77 Thalamus_L
78 Thalamus_R
79 Heschl_L
80 Heschl_R
81 Temporal_Sup_L
82 Temporal_Sup_R
83 Temporal_Pole_Sup_L
84 Temporal_Pole_Sup_R
85 Temporal_Mid_L
86 Temporal_Mid_R
87 Temporal_Pole_Mid_L
88 Temporal_Pole_Mid_R
89 Temporal_Inf_L
90 Temporal_Inf_R

CURRICULUM VITAE

JARED GRANT HESSE
hessjg14@wfu.edu

EDUCATION

Florida Atlantic University – Harriet L. Wilkes Honors College
Bachelor in Liberal Arts with a Concentration in Psychology **2010-2014**
Graduated Cum Laude (GPA 3.66)
Honors Thesis: *The Network Structure of the History of Personality Psychology*
Kenan Social Engagement Scholar (2012)
Bigony Pay-It-Forward Scholar (2012-2014)
Named Scholar (2012-2014)

Wake Forest University
M.A. in Psychology with a Concentration in Cognitive Psychology **2014-2016**

RESEARCH EXPERIENCE

Wake Forest University, Winston-Salem, NC
Graduate Assistant (Dagenbach Lab) **2014-2016**
Worked with network science approaches to cognitive research questions. Currently looking at how neural network efficiency measures relate to processing speed, in collaboration with the Laboratory for Complex Brain Networks.
Research Group Leader: Dale Dagenbach, Ph.D.

Wake Forest Baptist Medical Center, Winston-Salem, NC
Senior Research Team Member (Neurology) **2014-2016**
Analyzed fMRI data of Parkinson's patients at rest and during gambling tasks to investigate impulsivity in PD. Coordinated meetings, journal clubs, and oversaw the initiation and maintenance of several neurological investigations into Parkinson's.
Research Group Leader: Ihtsham ul Haq, M.D.

Harriet L. Wilkes Honors College, Jupiter, FL

Principal Investigator **2014**

Investigated how network analysis can describe the structure of personality psychology throughout history. Longitudinally analyzed over 3,000 citations from the Annual Review of Psychology in a 20,000 node citation network. Articulated how personality psychology has changed over time with network measures such as modularity and PageRank.

Faculty Advisor: Kevin Lanning, Ph.D.

EXTRACURRICULAR INVOLVEMENT

Student Government Chief of Staff, Harriet L. Wilkes Honors College of FAU (2013-2014)

Student Government Senator, Harriet L. Wilkes Honors College of FAU (2011)

Elections Commissioner, Harriet L. Wilkes Honors College of FAU (2010-2012)

Orientation Week Leader, Florida Atlantic University (2010-2014)

PUBLICATIONS, POSTERS, AND SYMPOSIA

Rothstein, A., Avery, B., Boyanpally, A., Hesse, J., Coghill, R., Laxton, A., Tatter, S., Siddiqui, M., & Haq, I. (2015, June). *Symptom severity and pain intensity may be risks for post STN DBS impulsivity in Parkinson's disease*. Poster presented at the 19th International Congress of Parkinson's Disease and Movement Disorders, San Diego, CA.

Sollman, M., Haq, I., Kramer, S., Cook, J., Hesse, J., Siddiqui, M., Laxton, A., & Tatter, S. (2015, June). *Limitations of the BDI-II in PD evaluations: Concordance with the GDS-30.* Poster presented at the 19th International Congress of Parkinson's Disease and Movement Disorders, San Diego, CA.

Hesse, J., & Lanning, K. (2014, May). *Meaningful links: Using network analysis to articulate the structure of personality psychology*. Poster presented at the 2014 Harriet L. Wilkes Honors College Symposium, Jupiter, FL.

Lanning, K., Sherman, R., Zhu, X., Hesse, J., & Lopez, D. (2014, May). *The new empiricism: Big data, network science, and psychological inquiry; Beyond keywords: Network analyses of psychological science*. Symposium presented at the 26th Annual Convention for the Association for Psychological Science, San Francisco, CA.

Goldstein, J., Hesse, J., Ricketts, K., Rohan, R., Sax, S., & O'Brien, W. (2014, April). *Searching for the truth*. Video presented at the 2014 Harriet L. Wilkes Honors College Symposium, Jupiter, FL.